

Document downloaded from:

<http://hdl.handle.net/10251/186854>

This paper must be cited as:

Macian Martinez, V.; Luján, JM.; Climent, H.; Miguel-García, J.; Guilain, S.; Boubennec, R. (2021). Cylinder-to-cylinder high-pressure exhaust gas recirculation dispersion effect on opacity and NOx emissions in a diesel automotive engine. *International Journal of Engine Research*. 22(4):1154-1165. <https://doi.org/10.1177/1468087419895401>



The final publication is available at

<https://doi.org/10.1177/1468087419895401>

Copyright SAGE Publications

Additional Information

# Cylinder to cylinder HP EGR dispersion effect on opacity and NOx emissions in a diesel automotive engine

Vicente Macián<sup>a</sup>, José Manuel Luján<sup>a</sup>, Héctor Climent<sup>a\*</sup>, Julián Miguel-García<sup>a</sup>, Stéphane Guilain<sup>b</sup>, Romain Boubennec<sup>b</sup>

<sup>a</sup> CMT Motores Térmicos, Universitat Politècnica de València, Spain

<sup>b</sup> Renault S.A. - Lardy - France

\*Corresponding author: [hcliment@mot.upv.es](mailto:hcliment@mot.upv.es). Telephone: (+34) 96 387 76 50. Postal address: CMT Motores Térmicos. Universitat Politècnica de València. Camino de Vera s/n. 46022. Valencia. Spain.

## Abstract

The objective of the study is to determine the effect of the high pressure exhaust gas recirculation (HP EGR) dispersion in automotive diesel engines in NOx and smoke emissions in steady engine operation. The investigation quantifies the NOx and smoke emissions as a function of the dispersion of the HP EGR among cylinders.

The experiments are performed on a test bench with a 1.6 liter automotive diesel engine. In order to track the HP EGR dispersion in the intake pipes, a valves system to measure CO<sub>2</sub>, hence EGR rate, pipe to pipe was installed. In addition, a valves device to measure NOx emissions cylinder to cylinder in the exhaust was installed. Moreover a smoke meter device was installed downstream the turbine, to measure the effect of the HP EGR dispersion on smoke emissions. Five different engine speeds were studied with different torque levels thus the engine map was widely studied, from 1250 to 3000 rpm and between 6 and 20 bar of **brake mean effective pressure** (BMEP). The EGR rate variates between 4 and 25 % depending on the operation point.

The methodology was focused in experimental tools combining traditional measuring devices with a specific valves system, which offers accurate information about species concentration in both the intake and the exhaust manifolds. The study was performed at constant raw NOx emissions to observe the effect of the EGR dispersion in the opacity **and fuel consumption**.

The study concludes that when the EGR dispersion is low, the opacity presents reduced values in all operation points. However, above a certain level of EGR dispersion, the opacity increases dramatically with different slopes depending on the engine running condition. This study allows quantifying this EGR dispersion threshold. In addition, the EGR dispersion could contribute to increase the fuel consumption up to 3.5%.

## 1. Introduction

In the last years the focus is over diesel engines emissions, especially smoke but NOx too. During past decades a lot of technologies and strategies have been developed to reduce the emissions and comply the regulations. One of the most famous and popular strategy to reduce NOx emissions in diesel automotive engines is the EGR [1, 2]. As the regulation according on NOx emissions advances, the strategies become more complex [3] and the EGR rates increase [4]. The EGR inhibits the NOx formation mainly due to

43 the reduction of the peak combustion temperature and the oxygen concentration as  
44 explained by Ladommatos et al. in 1996 and 1997 [5-8]. The benefits of EGR are  
45 observed on other applications like industrial natural gas engines [9]. However, the EGR  
46 strategies present some disadvantages such as the increase of smoke levels [10]. There  
47 is a compromise between smoke and NO<sub>x</sub> emissions, which are inversely related.

48 Moreover, the forecast in emissions legislation is the incorporation of new restrictions at  
49 low temperatures and high altitudes [11]. According to the new restrictions Xavier Tauzia  
50 et al. presented a detailed study in 2018 [12] related to the effect of cold starting  
51 temperatures, between 30°C and 90°C, over the efficiency because of the friction and  
52 the heat transfer during the thermal transient, moreover the combustion efficiency  
53 decrease due to higher CO and HC emissions at low load. Moreover pollutant emissions  
54 are highly effected because of the temperature variation of 60°C where CO, HC and soot  
55 evolution is complex although the NO<sub>x</sub> decrease at low temperatures. Finally, low  
56 coolant temperature is more determinant than oil temperature which only affects to  
57 friction losses, nevertheless it should be considered too. From this point of view, the EGR  
58 strategies are very interesting to reduce the pollutant emissions, especially HP EGR to  
59 start the engine at low temperatures as J.M. Luján et al. studied in 2018 [13]. New  
60 homologation cycles including transient operation to approach to real engine working  
61 conditions like the Worldwide Harmonized Light vehicles Test Procedures cycles [14]  
62 and World Harmonized Transient Cycle. From this point of view, the EGR strategies must  
63 be optimized to adapt itself to these working conditions and comply the legislation [15].

64 EGR system is not the only strategy to reduce NO<sub>x</sub> emissions. Nowadays there are new  
65 after-treatment systems such as Selective Catalytic Reduction (SCR) based on Urea  
66 Water Solutions (UWS) which react with NO<sub>x</sub> in the exhaust when the solution is injected.  
67 The reaction reduces the NO<sub>x</sub> emissions notably. This system is adapting to the new  
68 requirements like the World Harmonized Transient Cycle, commented before. It is being  
69 applied to diesel engines in transient operations by a specific thermal management since  
70 the catalyst activity decreases significantly if the exhaust temperature is lower than  
71 200 °C [16] or higher than 500 °C. In addition, this system presents a problem of thermal  
72 aging because of the high temperatures of the exhaust gases. Moreover SCR is low  
73 effective in urban areas because the temperature in the exhaust is usually lower than  
74 200 °C.

75  
76 Other problem presented by this system is the poisoning due to the sulfur content in the  
77 fuel, unburned hydrocarbons and Pt-Pd from the Diesel Oxidant Catalyst (DOC) and  
78 Diesel Particulate Filter (DPF) which is explained by Bin Guan et al. in a review of the  
79 state of the art technologies of SCR in 2014 [17]. More disadvantages are presented by  
80 this system like the deposits of urea and its byproducts during cold weather conditions  
81 and low exhaust temperature [18]. Furthermore this control penalizes the fuel  
82 consumption far than idle speed because of the increase of the backpressure. The  
83 control implies an increment of urea consumption too and it is mandatory to take into  
84 account the economic spending to load the tank with UWS. Finally this system presents  
85 economical disadvantages compared to EGR.

86  
87 So, the development of new and more complex EGR strategies are necessary because  
88 of the reduction emissions requirement, the economic cost of the after-treatment systems

89 and the problems commented before. Studies like Millo et al. in 2012 and Zamboni et al.  
90 in 2013 present results about the simultaneous use of HP and LP EGR as an effective  
91 combination to reduce NOx emissions and fuel consumption at low and medium speed  
92 and load conditions [19, 20]. In addition, HP and LP EGR have different consequences  
93 on the engine performance depending on the operation point [21] so both are necessary  
94 but the use of one loop or the other will depend on the needs. A recent updated study  
95 authored by Magín Lapuerta et al. in 2018 analyzed deeply the applications of LP EGR  
96 and HP EGR depending on the needs in a Euro 6 diesel engine equipped with DOC, a  
97 lean-NOx trap and DPF [22].

98  
99 This study is focused in the HP EGR configuration. In one hand, HP EGR shows some  
100 disadvantages compared to LP EGR [23]. HP EGR reduces NOx emissions but  
101 penalizing the fuel consumption and the dispersion of the EGR among cylinders, as it  
102 was commented before, which increase the smoke and NOx emissions. In other hand,  
103 HP EGR presents some advantages versus LP EGR. HP EGR is faster than LP EGR  
104 because of the length of the line, which is closer to the intake manifold. It produces less  
105 HC emissions too and its efficiency is higher at cold conditions due to the increase of the  
106 temperature [24]. In addition, HP configuration needs less exhaust energy because the  
107 compressor operates under lower amount of gas. Moreover, the LP EGR presents  
108 troubles related to condensation issues at low ambient temperatures when it mixes with  
109 ambient air, this effect was recently studied by J. R. Serrano et al. in 2018 and J. Galindo  
110 et al. in 2019 to predict the condensation rate [25] and its effect in the rotor of the  
111 compressor [26] respectively. Nevertheless, at low ambient temperature, condensation  
112 issues can be appear in whole engine and in all its elements, in the HP EGR line for  
113 instance like J. M. Luján et al. described in 2019 [27].

114  
115 The effect of the dispersion of HP EGR between cylinders on smoke and NOx emissions  
116 in automotive diesel engines is a topic to explore in depth. Long time ago emissions  
117 troubles related to unequal distribution between cylinders or bad mixing of the HP EGR  
118 were widely known and strategies to minimize that effect were developed by Robert et  
119 al. and William et al. in 2001 and 2002 respectively [28, 29]. Furthermore in 2009  
120 Maiboom et al. performed a study about the increment of the NOx and PM emissions as  
121 consequences of an unequal cylinder-to-cylinder EGR distribution and increasing the  
122 EGR rate [30]. The efficiency related to the NOx-PM trade-off of LP and HP EGR system  
123 was studied too in 2010 by Maiboom et al. [31] and Payri et al. [32]. Nowadays it is  
124 evident that both of loops are useful depending on the situation and, although it was  
125 concluded that LP EGR has more advantages to reduce emissions, it was not very clear  
126 how much more.

127  
128 In 2013 Lakhani et al. [33] studied the cylinder to cylinder HP EGR dispersion with  
129 experimental and modelling tools in light-duty trucks and the effect on NOx-PM trade-off.  
130 The study compares the same operation points with and without HP EGR mixture. The  
131 study concludes that the effect of the dispersion in PM and NOx trade-off is significant in  
132 partial and high loads; however, the impact at low loads remains unclear. Moreover, the  
133 EGR mixture has a negligible effect on combustion. In 2015 Dimitriou et al. [34]  
134 performed an analysis of the cylinder to cylinder dispersion by 1D and 3D modelling  
135 tools. The study was focused in the parameters and effects that enhance the air-EGR  
136 mixing behavior like turbulence, Venturi, air-EGR contact area and the size and number

137 of injection ports of EGR. The study concluded that velocity, turbulence, Venturi effect  
138 and a lot of small ports in the mixer improve the air-EGR mixing. An experimental study  
139 developed by Luján et al. in 2015 [35] demonstrated that the reduction of EGR dispersion  
140 is related with a significant reduction of NOx emissions and the effects on fuel  
141 consumption are negligible.

142

143 The main outcome of this work is to quantify the relationship between opacity and fuel  
144 consumption with the EGR dispersion in several engine running conditions in a state of  
145 the art diesel automotive engine. This information provides relevant information in order  
146 to design engine components to reduce the emissions caused by HP EGR dispersion.  
147 Experimental tools were used in this study, combining traditional and ad-hoc devices, to  
148 develop a methodology to promote different EGR dispersion levels so as to assess the  
149 impact in engine performance.

150

151 The paper is structured as follows: In Section 2 the experimental setup is explained.  
152 Section 3 contains main results and discussion in terms of dispersion and its influence  
153 on smoke and fuel consumption. Finally, main conclusions are presented in Section 4.

154

## 155 2. Experimental setup

156 The experiments are performed on a test bench with a turbocharged diesel engine. Table  
157 1 shows the main features of the engine. The engine includes both LP and HP EGR  
158 systems. This study is focused only in the HP EGR loop of the engine, whose schematic  
159 layout is depicted in Fig. 1. The original configuration was modified since it is necessary  
160 to measure the CO<sub>2</sub> concentration in each intake pipe of the cylinders and control the  
161 dispersion of the EGR meticulousness.

### 162 Table 1

163 Engine specifications.

---

Cylinder number	In-line 4
Bore x stroke (mm)	80x79.5
Displacement (cm <sup>3</sup> )	1600
Compression ratio	15.4:1
Valve number	4/cylinder
Fuel delivery system	Common rail. Direct injection.
EGR system	HP EGR and LP cooled EGR
Intake boosting	Turbocharger with VGT
Intake cooling system	Air charge air cooler (ACAC)
Maximum power (kW/rpm)	96/4000
Maximum torque (Nm/rpm)	320/1750

164

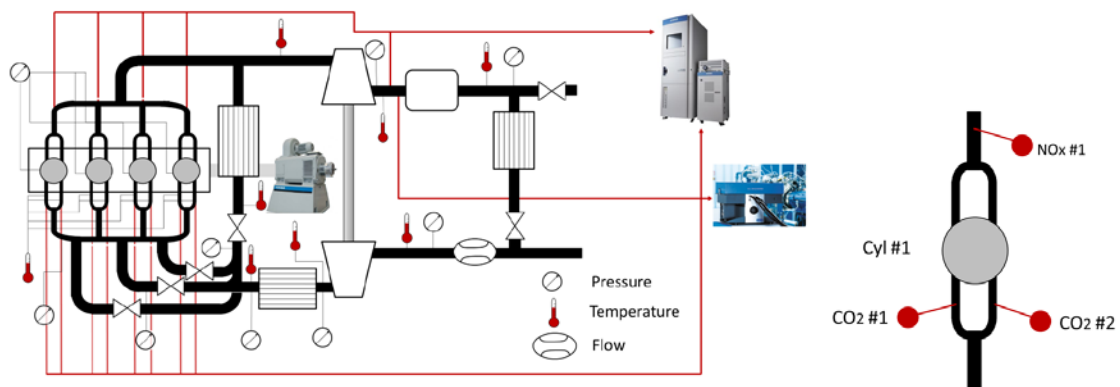
165 Firstly, a specific hardware, composed by valves and probes, was installed to determine  
166 the dispersion of the EGR rate in the intake and the dispersion of the NOx emissions in  
167 the exhaust. Up to nine probes were installed in the intake and five in the exhaust  
168 manifold. The probes were connected to a Horiba MEXA 7170DEGR, which is a  
169 conventional gas analysis system widely used in engine testing in steady conditions.  
170 Each probe had a valve that controls the gases flow to the gas analyzer. Usually, one of

171 the valves was opened meanwhile the others were closed to measure only the gas  
 172 composition from one pipe. During the measurement in the intake manifold, the valves  
 173 of the exhaust were all closed and in reverse, during the measurement in the exhaust,  
 174 the valves of the intake were all closed.

175 The configuration in the intake was one probe for each intake pipe, two per cylinder, and  
 176 one to take air from the environment to perform the change of the acquisition between  
 177 pipes. It is not possible to close one valve and open another after that because the  
 178 acquisition system is breathing continuously and it would generate vacuum and it could  
 179 break the measuring device. For this reason, it is necessary to open first another valve  
 180 and then close the previous one. The ninth probe measured the ambient gas  
 181 composition, so it measured a very low CO<sub>2</sub> level. The configuration in the exhaust is  
 182 similar: five probes were installed in the exhaust, one per cylinder and one to measure  
 183 the total value downstream of the turbine.

184 Furthermore, a specific manufactured device was installed between the HP EGR line  
 185 and the intake manifold with three pipes and three regulation valves (one per pipe) to  
 186 control the HP EGR dispersion. The pipes were distributed in the intake manifold to  
 187 encompass it. One pipe was located on the left, other was located on the right and the  
 188 third was located on the center, on the top of the manifold, as in the original configuration.  
 189 Each pipe contained a regulation valve to control the HP EGR dispersion with high  
 190 accuracy as it is observed in the following figure.

191



192

193 **Figure 1.** Engine schematic layout and emissions measurement detail in the cylinders

194 Different sensors were installed additionally to measure different engine parameters,  
 195 which help to set the steady engine conditions to perform the tests. They also offer a lot  
 196 of information to process properly the results. The variables together with the sensors  
 197 features are presented in Table 2.

198 Table 2

199 Instrumentation accuracy

Sensor	Variable	Accuracy [%]	Range
--------	----------	--------------	-------



Thermocouples type K	Temperature	1	0 °C – 1260 °C
Pressure sensor	Pressure	0.3	0 - 6 bar
Pressure sensor	Pressure	0.05	0-150 bar
Gravimetric fuel balance	Fuel mass flow	0.2	0 - 150 kg/h
Hot wire meter	Air mass flow	1	0 - 720 kg/h
Dynamometer brake	Torque	0.1	0 - 480 Nm
Smoke Meter	Soot	0.5	0 – 32000 mg/m3

200

201 Engine tests in steady conditions were performed to analyze the dispersion of the HP  
 202 EGR and its effect on the NOx and smoke emissions. First, it was necessary to determine  
 203 the operating points taking care to study a large range in the engine map. Initially, five  
 204 different engine speeds were defined with different Brake Mean Effective Pressure  
 205 (BMEP). After that, the EGR rate was determined under two restrictions: the first one  
 206 was to study a large range between low and medium EGR rate, and the second one was  
 207 to keep margin to be able to modify the HP EGR dispersion taking into account the effect  
 208 on the engine stability, highly affected when the air to fuel ratio approaches to  
 209 stoichiometric conditions. Finally, the EGR rate to perform the study was determined as  
 210 a function of the emissions and the stability. The final engine running conditions are  
 211 presented in Table 3.

212 Table 3

213 Working operation points

N [rpm]	BMEP [bar]	Intake P [mbar]	EGR rate [%]	Engine Torque [Nm]
1250	11	1500	6	140.1
1500	15	1900	5	191
2000	6	1250	23	76.4
2500	11.7	2300	20	149
3000	20	2750	11	254.6

214

215 In each operating point, the values shown in Table 3 had to be kept constant so the  
 216 control strategy during the tests was based on three different engine controls at steady  
 217 conditions. The first one was the engine torque, which was controlled by the injected fuel.  
 218 The second one was the intake manifold pressure, which was controlled by the Variable

219 Geometry Turbine (VGT) position. And the third one was the NOx emissions which were  
220 controlled with the EGR rate, hence the HP EGR valve position.

221 The process to perform the tests was always the same for every operation point. The  
222 configuration of the three valves to control the HP EGR dispersion was set before starting  
223 the engine. After that, the engine was started and the operation point was set (speed,  
224 torque, intake manifold pressure and NOx emissions level). It was necessary to wait to  
225 stabilize the temperature of the engine to take real steady conditions. The testing  
226 procedure started with the acquisition of CO<sub>2</sub> concentration in the intake pipes and intake  
227 air sequentially. It required a few seconds to stabilize the measurement and obtain an  
228 accurate result, between ten and twenty seconds per pipe, depending on the working  
229 operation point.

230 After the registration in the intake line, the measurement of the NOx emissions in the  
231 exhaust manifold takes place. The procedure is similar to the previous one. Only one  
232 valve was open simultaneously except when the measurement probe was changed to  
233 avoid the vacuum effect. As in the intake, it is essential to wait a few seconds to stabilize  
234 the measurement. In this case, the duration is longer than before, between one or two  
235 minutes for each cylinder depending on the working operation point.

236 The opacity could be measured anytime, independently of the registration of other  
237 variables. It was measured with a traditional measuring device such as the AVL Smoke  
238 Meter 415S. It only needed a few seconds to take a precise measure each time. Horiba  
239 MEXA 7170DEGR is the equipment that measures the pollutant emissions, except  
240 opacity. It acquires the CO, CO<sub>2</sub>, THC, O<sub>2</sub> and NOx concentrations. It is not possible  
241 measure the EGR rate directly, so it is necessary a conversion from exhaust and intake  
242 CO<sub>2</sub> concentration measurements [36] following the next expression:

$$EGRrate = \frac{[CO_2]_{Intake} - [CO_2]_{Ambient}}{[CO_2]_{Exhaust} - [CO_2]_{Ambient}} \quad (1)$$

### 243 3. Results and discussion

244 Once it has been explained the experimental tools, it is possible to analyze and discuss  
245 the results in terms of engine performance, emissions and HP EGR dispersion levels.

246 Fig. 2 shows the intake manifold pressure on the left and the engine torque on the right  
247 related to the nominal value presented in Table 3. The 2000 rpm engine operating  
248 condition is shown. The other operation points present similar results. The x-axis  
249 represents the standard deviation of the EGR following the next expression:

$$\sigma_{EGR} = \sqrt{\frac{\sum_{i=1}^n (x_i - \bar{X})^2}{n}} \quad (2)$$

250 Where:

251  $i$  = the number of the cylinder.

252  $n$  = 4 (total number of cylinders).

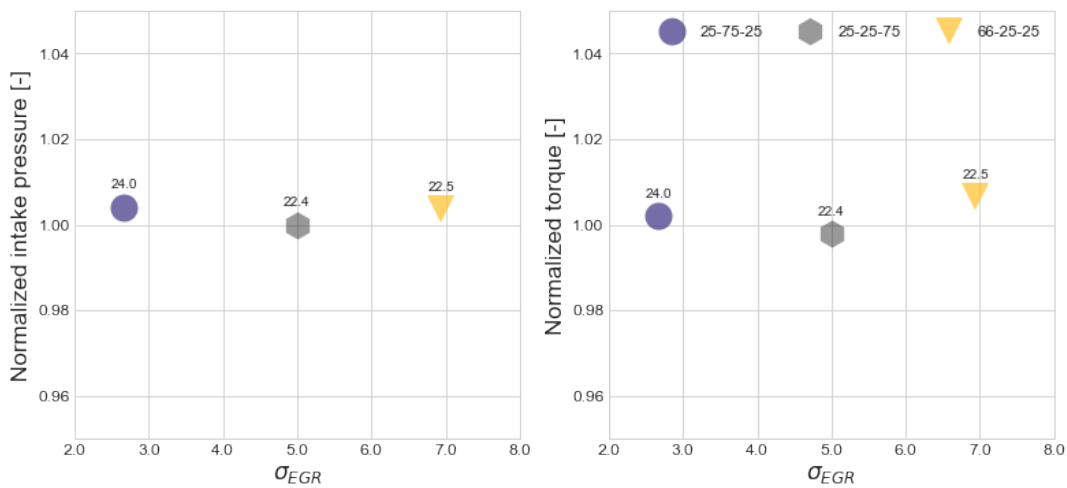


253  $x_i$  = the average CO<sub>2</sub> concentration in cylinder i.

254  $\bar{x}$  = the average CO<sub>2</sub> concentration in the 4 cylinders.

255 It is possible to observe in the graph on the right the legend of the working operation  
256 points. The numbers represent the position of the three regulation valves of the EGR,  
257 where 0% means that it is completely closed and 100% is completely open. The number  
258 on the left represents the left valve before the manifold (in the sense of the flow), the  
259 number in the center represents the center valve and the number in the right represents  
260 the right valve, as depicted in Fig. 1. Over the **dots**, the EGR rate in each test is shown.  
261 It is possible to see that all of them are under 3% of variation, in both variables, intake  
262 manifold pressure and engine torque. In summary, during the testing campaign, although  
263 the HP-EGR dispersion was modified, all the tests were performed keeping nearly  
264 constant values of intake manifold pressure (by fine tuning the VGT opening) and engine  
265 torque (by modifying the injected fuel). For the sake of paper brevity, only the 2000 rpm  
266 results are shown.

267



268

269 Figure. 2. Intake manifold pressure and engine torque referenced to the nominal value  
270 at 2000 rpm engine conditions.

271 Fig. 3 presents the NO<sub>x</sub> values related to the average value for each engine running  
272 condition, measured in the exhaust manifold to take the information per cylinder  
273 (numbered from 1 to 4) and downstream the turbine to measure the raw NO<sub>x</sub> emissions  
274 value (named T). The four plots rows correspond to the 1500, 2000, 2500 and 3000 rpm  
275 engine running conditions. The x-axis represents the EGR rate on the plot on the left,  
276 and the EGR standard deviation on the right. The left plot shows the effect of the EGR  
277 in the NO<sub>x</sub> emissions, cylinder to cylinder, and in the engine. The plot on the right shows  
278 the engine raw NO<sub>x</sub> as a function of the standard deviation of the EGR. The average  
279 EGR rate is labelled above the dots.

280 Paying attention, for example, to 3000 rpm working operation point it is possible to  
281 observe that the case with the lowest standard deviation (50-100-50) has a very similar  
282 EGR rate value in each cylinder. From left to right, in the sense of the flow, the cylinders  
283 1, 2 and 3 have an EGR rate very close to the nominal value, 11%, and cylinder 4 has a

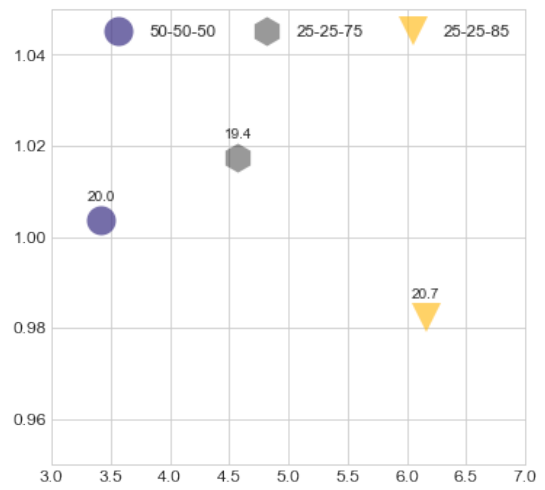
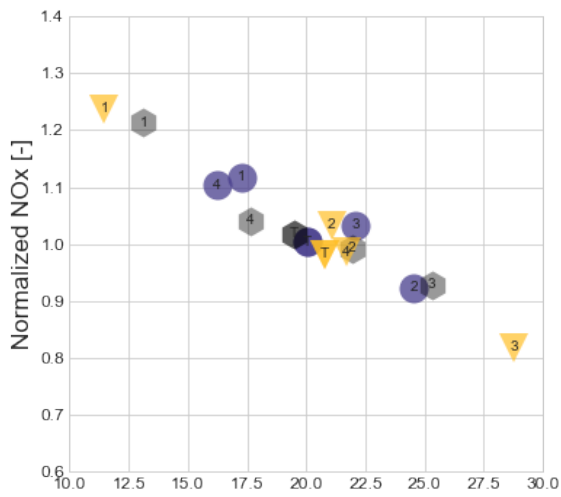
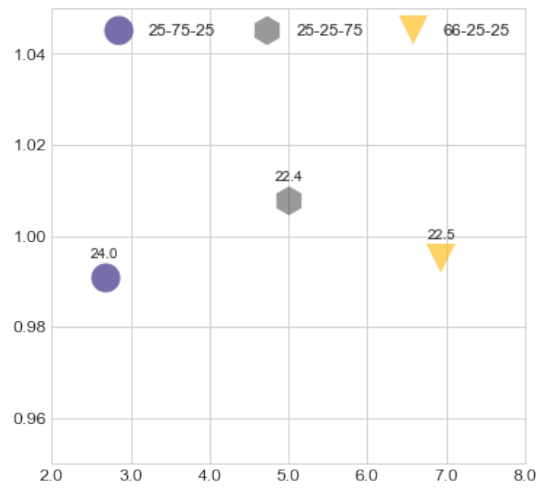
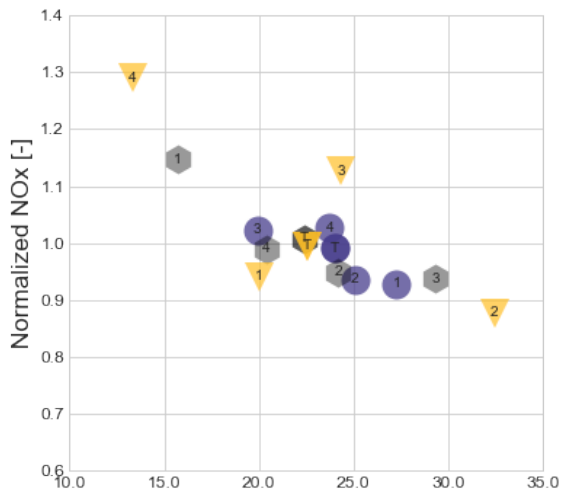
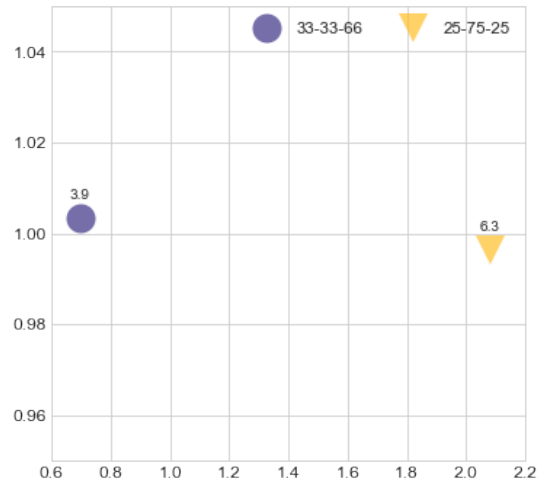
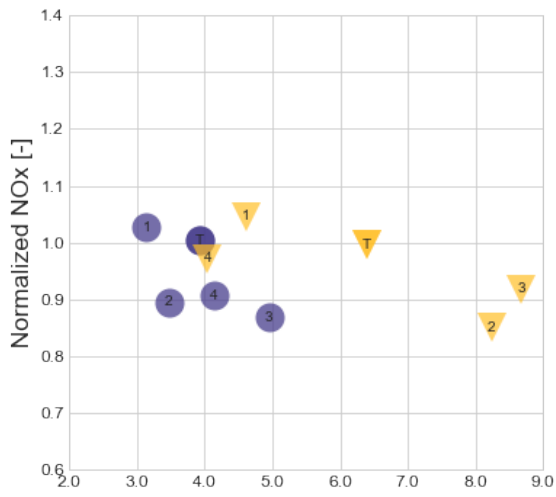
284 little bit more, close to 12%, what represents an increment of the 9% approximately  
285 referred to the nominal value.

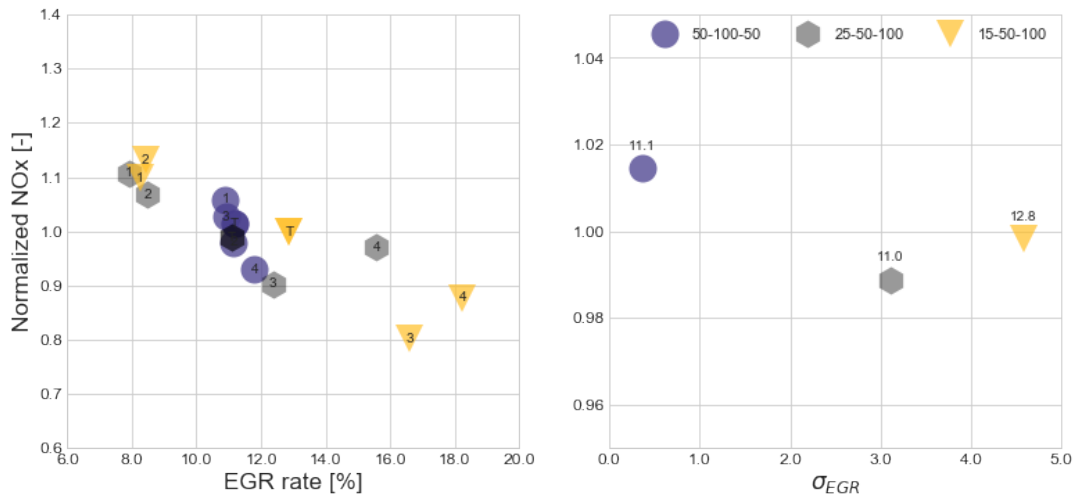
286 The second case (25-50-100) presents a higher value of standard deviation where the  
287 cylinder 1 and 2 has 8% and 8.5% EGR rate, the cylinder 3 has 12.5% and cylinder 4  
288 has 15.5% EGR rate. In this **case**, the minimum and the maximum EGR rate represents  
289 a reduction of 27% and an increment of 41% respectively.

290 In the last case, with the highest standard deviation, cylinders 1 and 2 have similar values  
291 of EGR rate than the second case (between 8% and 8.5%), cylinder 3 has 16.5% and  
292 cylinder 4 close to 18.5% EGR rate. **Cylinder 4 shows the most dramatic increase of the**  
293 **EGR rate, cylinder 4 presents an increment of 68% referred to the nominal value (11%).**  
294 **Moreover, particularly in this case, 15-50-100, with the highest standard deviation, the**  
295 **average EGR rate is slightly higher than nominal value, 12.8% instead 11%. Even with**  
296 **this increase in the average EGR rate, 12.8%, the increment in cylinder 4 is 44% higher,**  
297 **which is the highest difference in any case at 3000 rpm.** It is possible to observe that a  
298 higher standard deviation means a large difference in terms of EGR rate between  
299 cylinders. In this case, the difference between the lowest and the highest EGR rate per  
300 cylinder is close to **10 points**, from 8% on cylinder 1 to slightly more than 18% on cylinder  
301 4.

302 Although each cylinder and each case presents different values of EGR rate and  
303 standard deviation respectively, all the cases were performed at constant NO<sub>x</sub> level for  
304 the same working operation point. In some cases, it was necessary to increase the EGR  
305 rate, to keep the same NO<sub>x</sub> value. An example was commented before, where the third  
306 case at 3000 rpm (15-50-100) reveals an average EGR rate of 12.8% instead of 11%.  
307 While the two cases with less EGR standard deviation presented a similar value to the  
308 nominal setup.

309 This effect is observed too at 1500 rpm working operation point and it is not at 2000 and  
310 2500 rpm. 3000 and 1500 rpm operation points have in common a low average EGR  
311 rate (lower than 23% and 20% presented by 2000 and 2500 rpm operation points  
312 respectively). In all the situations, a 2% difference in NO<sub>x</sub> level is accepted when  
313 controlling the EGR valve at the engine operating condition between the different  
314 dispersion valves configurations.



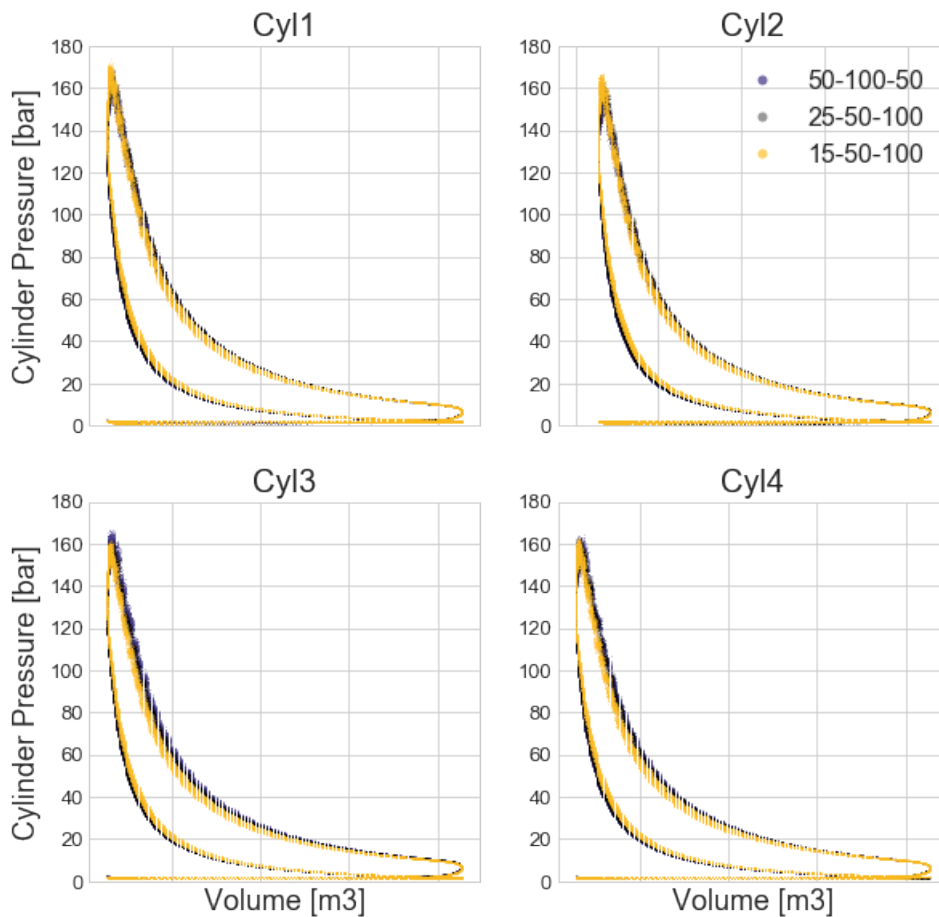


318

319 Figure 3. Cylinder and engine NOx values vs. EGR rate (left), and engine raw NOx vs.  
 320 EGR standard deviation (right) for the 1500, 2000, 2500 and 3000 rpm operation points  
 321 (from top to bottom).

322 In order to check the influence of the EGR dispersion in the in-cylinder pressure traces,  
 323 Fig. 4 shows several consecutive engine cycles measured in all cylinders. In this  
 324 particular case, the 3000 rpm situation is plotted with three different HP EGR dispersion  
 325 levels, as the legend shows in the top of the figure on the right. The numbers represent  
 326 the position of the regulation valves to control the dispersion as explained before.

327 It is very difficult to derive any conclusion from direct in-cylinder pressure inspection  
 328 because the p-V diagram is practically the same in all cases. It is not possible to appraise  
 329 significant differences between case and case and between cylinder and cylinder due to  
 330 the negligible differences, so the calculation of the Indicated Mean Effective Pressure  
 331 (IMEP) values are provided in Fig. 5 for several cases.



332

333 Figure 4. In-cylinder pressure vs cylinder displacement for all the cylinders and three  
 334 different dispersion levels at 3000 rpm.

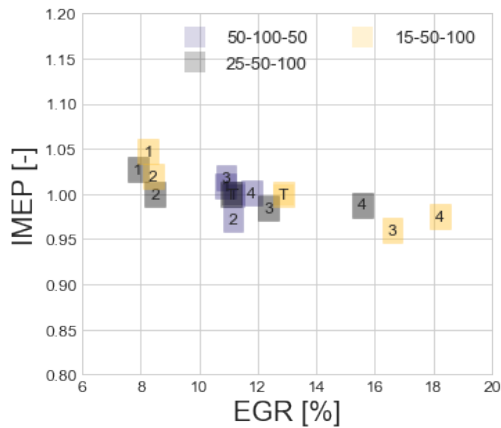
335 Fig. 5 shows the IMEP (dimensionless with the average) for all the cylinders (numbering  
 336 from 1 to 4) and the average (named T) as a function of the EGR rate at 3000 rpm, as in  
 337 Fig. 4. It is possible to observe that the dispersion affects to the IMEP of the cylinders  
 338 (individually). Since the tests are performed keeping the engine torque constant, the  
 339 average of the IMEP is not modified. In addition, the IMEP variation range, per cylinders,  
 340 is lower than 5% most of times. Therefore, it is possible to affirm that the influence of the  
 341 EGR dispersion to the IMEP of the cylinders is very limited.

342

343

344

345



346

347 Figure 5. Dimensionless IMEP for all the cylinders (numbered from 1 to 4) and the  
 348 average (named T) versus EGR rate for three different HP EGR dispersion levels at 3000  
 349 rpm.

350 Fig. 6 shows the air to fuel ratio measured in the exhaust gases (i.e. lambda), the  
 351 adimensional brake specific fuel consumption (BSFC) that is calculated as the ratio  
 352 between the BSFC and the BSFC achieved with the lowest EGR dispersion at the given  
 353 engine running condition, and the exhaust gases opacity as a function of the EGR  
 354 dispersion in all the engine running conditions (1250, 1500, 2000, 2500, 3000 rpm) and  
 355 all the dispersion levels.

356 A reduction on the lambda values is observed as EGR dispersion increases, which can  
 357 be explained mainly by two reasons: either changes in the air mass flow entering the  
 358 cylinders or variations in the injected fuel. As already discussed in Fig. 3, an increment  
 359 of EGR rate was necessary to maintain the NOx nominal value in the 1500 and 3000  
 360 rpm engine running conditions. The difference between these working operation points  
 361 and the other, 2000 and 2500, was the EGR rate. The former points have lower EGR  
 362 rates, around 5-10%, while the latter points have higher EGR rates, over 20%. On the  
 363 other hand, regarding the fuel injection, more fuel quantity is needed when the EGR  
 364 dispersion increases in the 2500 and 3000 rpm running conditions, which is easily  
 365 detected in the BSFC plot. This means that the impact of the EGR dispersion on the  
 366 combustion performance is more remarkable in these engine running conditions.

367 In Fig. 6 another difference related to lambda value is detected: the engine running  
 368 conditions at 1500 rpm and 3000 rpm are close to engine full load operation and present  
 369 a lambda value lower than 1.25, while the other working operation points, 2000 rpm and  
 370 2500 rpm, present values over 1.3, corresponding to partial load situation. When the  
 371 engine approaches to stoichiometric conditions the combustion process in the cylinder  
 372 is more critical.

373 The 1250 rpm running condition, with two different EGR dispersion, needs to increase  
 374 the EGR rate, as the 1500 and 3000 rpm engine points, to keep the same NOx level.  
 375 These two points have an EGR rate of 6.2% and 7.1% in the low and high EGR  
 376 dispersion level respectively. The EGR absolute value is not very high but the difference  
 377 between both of them is considerable, around 14.5%. Moreover, this working operation  
 378 point presents low lambda values too, close to 1.2, since it is also close to full load  
 379 operation. Therefore, this point is very similar to 1500 and 3000 rpm operation points



380 due to the low EGR rate, the need to increase the EGR rate to keep the NO<sub>x</sub> level  
381 constant and the low lambda value.

382 On the other hand, the graph of the center presents a clear trend between the increment  
383 of BSFC and the increment of the EGR dispersion. The 3000 and 2500 rpm running  
384 conditions show the highest increment of the BSFC: 2.7%, from 1 to 1.027, and 3.5%,  
385 from 1.01 to 1.045, respectively. The 1250 and 2000 rpm running conditions present  
386 more modest increment than the other: 1.2%, from 1.124 to 1.138 and 1%, from 1.062  
387 to 1.071, respectively. Finally, the impact of the EGR dispersion on the specific  
388 consumption at 1500 rpm working conditions is very limited, at least in the range of the  
389 tested EGR dispersion.

390 To finish, the graph on the right shows a scatter plot where opacity increase significantly  
391 with the EGR dispersion. At 1250 rpm the opacity is 50% higher in the highest EGR  
392 dispersion dot than in the lowest, from 16 to 24%, but it is necessary to take into account  
393 that this effect could be not only caused because of the EGR dispersion but because of  
394 the increase of the EGR rate and the low lambda value too.

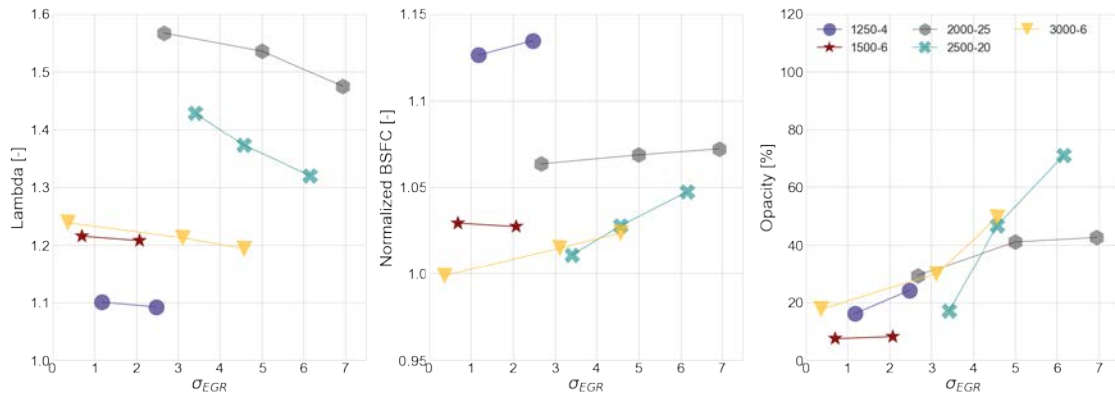
395 The data for 1500 rpm shows a very low increment between the two cases. It is the  
396 working operation point with the lowest EGR standard deviation. **Nevertheless**, it  
397 presents an opacity increment of 14% (from 7 to 8 %) but it is difficult to observe using  
398 the same y-axis scale than for the rest working operation points. In this case, as in 1250  
399 rpm, the absolute value of the EGR rate is low but there is an increment of EGR rate to  
400 keep NO<sub>x</sub> at constant level. As it was commented before in Fig. 3 where it was shown  
401 that the point with higher dispersion operates with an EGR rate of 6.3%, while the one  
402 with lower dispersion does with 3.9% EGR rate, which means an increment of 62%. In  
403 spite of the high increment of the EGR rate and the low lambda value, they have not big  
404 consequences in the opacity like at 1250 rpm.

405 The third case, 2000 rpm, is the first where the EGR rate does not increase with the EGR  
406 dispersion to keep the NO<sub>x</sub> level. **However**, it is possible to see a very clear trend: higher  
407 EGR dispersion between cylinders correlates with higher opacity levels. The opacity  
408 moves from 29% in the lowest EGR dispersion test to 42% in the highest case, which  
409 represents an increase around 45%.

410 The most extreme case correspond to the 2500 rpm engine running conditions where  
411 the opacity increase up to 70%, which means an increment close to 75% compared with  
412 the lowest opacity test. In fact, in addition to the high EGR rate that the engine is using  
413 in this point, the EGR rate in the cylinders presents huge differences, from 12% to 28%,  
414 higher than the lowest opacity point, which shows variations from 15% to 25%  
415 approximately.

416 Finally, the 3000 rpm case also presents high opacity values. As it was commented  
417 before, the engine runs with a low lambda value in this operation point. In the other hand  
418 the EGR rate of the highest EGR dispersion test is higher, 12.8%, than the others, 11%  
419 which could influence on the increase of the slope between the mid and high EGR  
420 dispersion tests, which translates into an increase of 150% among the lowest and highest  
421 EGR dispersion points.

422

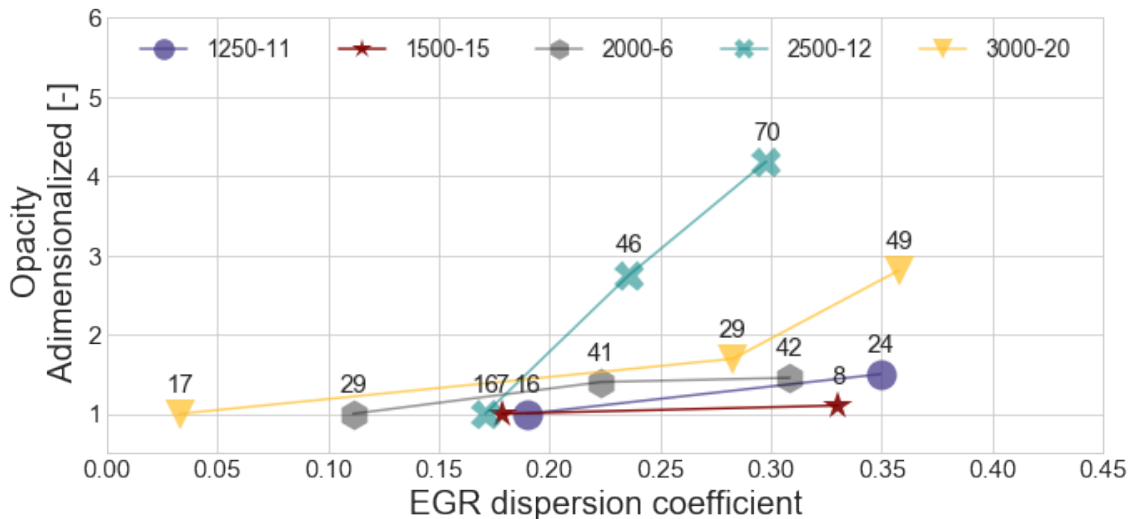


423

424 Figure 6. Lambda (left), BSFC (center) and opacity (right) vs EGR dispersion.

425 Fig. 7 gathers all the results in a single plot. Y-axis represents an adimensional opacity  
 426 that is calculated as the ratio between the opacity and the opacity achieved with the  
 427 lowest EGR dispersion at the given engine running condition. X-axis represents an  
 428 adimensional EGR dispersion index called EGR dispersion coefficient, which is  
 429 calculated as the ratio between the EGR standard deviation and the EGR rate. Over the  
 430 dots appears the actual opacity value in percentage. It is possible to realize that a  
 431 remarkable increase in the adimensional opacity appears for EGR dispersion coefficient  
 432 values higher than 0.2. Y-axis scale shows that, depending on the engine running  
 433 condition, the EGR dispersion phenomenon could multiply the opacity level for the lowest  
 434 EGR dispersion by a factor around 1 and 4.

435



436

437 Figure 7. Adimensional opacity vs EGR dispersion coefficient for all the tested engine  
 438 running conditions.

439 **4. Conclusions**

440 A novel methodology to study the HP EGR dispersion phenomenon was developed to  
 441 quantify the impact on engine performance and pollutant emissions. This methodology  
 442 is based on experimental tests on an automotive diesel engine where the intake manifold  
 443 was fully instrumented with CO<sub>2</sub> probes together with a special hardware to modify and

444 control the EGR dispersion between cylinders. The study includes a wide set of engine  
445 running conditions with different engine speed, engine torque and EGR rate. The tests  
446 were performed in five steady engine conditions where the EGR dispersion is modified  
447 but keeping constant the intake manifold pressure, the engine torque and the NOx raw  
448 emissions.

449 Depending on the engine running condition, it is necessary to increase the EGR rate to  
450 keep the NOx level constant when the EGR dispersion is varied. This usually happens  
451 when the engine runs with less than 15% EGR rate, while we found that it is not needed  
452 with EGR rates higher than 20%. Besides the EGR rate, other engine related parameters  
453 may influence on the results, being lambda one of the most important. If the engine runs  
454 near to stoichiometric situations, the conditions for remarkable increase of the opacity  
455 are likely to occur.

456 It is possible to conclude that the EGR dispersion affects to BSFC. As the EGR  
457 dispersion increases, the BSFC increases especially at high speeds, where the impact  
458 on the combustion process is more evident. A more thorough analysis is currently under  
459 investigation to find its causes.

460 Finally the standard deviation of the EGR rates for all the cylinders was converted to a  
461 non-dimensional figure taking into account the average EGR rate **resulting in** an EGR  
462 dispersion coefficient that helps to quantify the effect of the EGR dispersion on opacity  
463 emissions. The opacity was also transformed to a non-dimensional value using the  
464 opacity value of the test with the least dispersion. Both numbers were **plotted together**  
465 and it is possible to observe that the more affected points are 3000 and 2500 rpm running  
466 conditions followed by 1250 and 2000. It indicates that the influence of the lambda value  
467 and low EGR rate are not determinant on opacity emissions and the EGR dispersion has  
468 an important influence. So, finally, independently of the other factors, there is, always, a  
469 trend between the opacity and the EGR dispersion between cylinders. Attending to Fig.  
470 7, opacity may increase dramatically when the EGR dispersion coefficient exceeds 0.2.

## 471 **References**

472

473 1. Ming Zheng, Graham T. Reader, J. Gary Hawley. "Diesel engine exhaust gas  
474 recirculation – a review on advanced and novel concepts." Energy Conversion and  
475 Management 45 (2004) 883-900.

476 2. Deepak Agarwal, Shrawan Kumar Singh, Avinash Kumar Agarwal. "Effect of  
477 Exhaust Gas Recirculation (EGR) on performance, emissions, deposits, and  
478 durability of a constant speed compression ignition engine." Applied Energy 88  
479 (2011) 2900-2907.

480 3. A. Maiboom, X. Tauzia and J.-F. Hétet, "Influence of high rates of supplemental  
481 cooled EGR on NOx and PM emissions of an automotive HSDI diesel engine using  
482 an LP EGR loop." International Journal of Engine Research (2008); 32: 1383-1398.  
483 DOI: 10.1002/er.1455

484 4. A. Maiboom, X. Tauzia and J.-F. Hétet, "Experimental study of various effects of  
485 exhaust gas recirculation (EGR) on combustion and emissions of an automotive

- 486 direct injection diesel engine.” Energy 33 (2008) 22-34. Doi:  
487 10.1016/j.energy.2007.08.010
- 488 5. Ladommatos N, Abdelhalim SM, Zhao H, Hu Z. The dilution, chemical, and thermal  
489 effects of exhaust gas recirculation on diesel engine emissions – Part 1: Effect of  
490 reducing inlet charge oxygen. SAE paper 961165; 1996.
- 491 6. Ladommatos N, Abdelhalim SM, Zhao H, Hu Z. The dilution, chemical, and thermal  
492 effects of exhaust gas recirculation on diesel engine emissions – Part 2: Effects of  
493 carbon dioxide. SAE paper 961167; 1996.
- 494 7. Ladommatos N, Abdelhalim SM, Zhao H, Hu Z. The dilution, chemical, and thermal  
495 effects on exhaust gas recirculation on diesel engine emissions – Part 3: Effects of  
496 water vapor. SAE paper 971659; 1997.
- 497 8. Ladommatos N, Abdelhalim SM, Zhao H, Hu Z. The dilution, chemical, and thermal  
498 effects of exhaust gas recirculation on diesel engine emissions – Part 4: Effects of  
499 carbon dioxide and water vapor. SAE paper 971660; 1997.
- 500 9. Chris A Van Roekel, David T Montgomery, Jaswinder Singh, Daniel B Olsen,  
501 “Evaluating dedicated exhaust gas recirculation on a stoichiometric industrial natural  
502 gas engine” International Journal of Engine Research (2019)  
503 <https://doi.org/10.1177/1468087419864733>.
- 504 10. Tokura, N., Terasaka, K., and Yasuhara, S., "Process through which Soot Intermixes  
505 into Lubricating Oil of a Diesel Engine with Exhaust Gas Recirculation," SAE  
506 Technical Paper 820082, 1982
- 507 11. Vicente Bermúdez, José Ramón Serrano, Pedro Piqueras, Javier Gómez and  
508 Stefan Bender, “Analysis of the role of altitude on diesel engine performance and  
509 emissions using an atmosphere simulator.” International Journal of Engine  
510 Research 18 (1-2) (2017) 105-117. DOI: 10.1177/1468087416679569.
- 511 12. Xavier Tauzia, Alain Maiboom, Hassan Karky, Pascal Chesse, “Experimental  
512 analysis of the influence of coolant and oil temperature on combustion and  
513 emissions in an automotive diesel engine” International Journal of Engine Research  
514 20 (2) (2018) 247-260 <https://doi.org/10.1177/1468087417749391>.
- 515 13. José Manuel Luján, Héctor Climent, Santiago Ruiz and  
516 Ausias Moratal, “Influence of ambient temperature on diesel engine raw  
517 pollutants and fuel consumption in different driving cycles.” International Journal of  
518 Engine Research. DOI: 10.1177/1468087418792353.
- 519 14. José Galindo, Hector Climent, Olivier Varnier and Chaitanya Patil, “Effect of boosting  
520 system architecture and thermomechanical limits on diesel engine performance:  
521 Part II—transient operation.” International Journal of Engine Research 19 (8) (2017)  
522 873-885. DOI: 10.1177/1468087417732264.
- 523 15. José Manuel Luján, Héctor Climent, Francisco José Arnau, Julián Miguel-García,  
524 “Analysis of low-pressure exhaust gases recirculation transport and control in

- 525 transient operation of automotive diesel engines” Applied Thermal Engineering 137  
526 (2018) 184-192. <https://doi.org/10.1016/j.applthermaleng.2018.03.085>
- 527 16. Shuzhan Bai, Jianlei Han, Min Liu, Shunshun Qin, Guihua Wang, Guo-xiang Li,  
528 “Experimental investigation of exhaust thermal management on NOx emissions of  
529 heavy-duty diesel engine under the world Harmonized transient cycle (WHTC)”  
530 Applied Thermal Engineering 142 (2018) 421-432,  
531 <https://doi.org/10.1016/j.applthermaleng.2018.07.042>.
- 532 17. Bin Guan, Reggie Zan, He Lin and Zhen Huang, “Review of state of the art  
533 technologies catalytic reduction of NOx from diesel engine exhaust” Applied Thermal  
534 Engineering, 66 (2014) 395-414.
- 535 18. Sadashiva Prabhu S, Nagaraj S Nayak, N Kapilan, Vijaykumar Hindasageri. “An  
536 experimental and numerical study on effects of exhaust gas temperature and flow  
537 rate on deposit formation in Urea-Selective Catalytic Reduction (SCR) system of  
538 modern automobiles.” Applied Thermal Engineering 111 (2017) 1211-1231
- 539 19. Federico Millo, Paolo Ferrero Giacominetto, Marco Gianoglio Bernardi, “Analysis of  
540 different exhaust gas recirculation architectures for passenger car Diesel engines”.  
541 Applied Energy 98 (2012) 79-91.
- 542 20. Zamboni, G., Capobianco, M., “Influence of high and low pressure and VGT control  
543 on in-cylinder pressure diagrams and rate of heat release in an automotive  
544 turbocharged diesel engine.” Applied Thermal Engineering 51 (2013) 586-596.
- 545 21. Shen, K., Li, F., Zhang, Z., Sun, Y., Yin, C., “Effects of LP and HP cooled EGR on  
546 performance and emissions in turbocharged GDI engine.” Applied Thermal  
547 Engineering 125 (2017) 746-755.
- 548 22. Magín Lapuerta, Ángel Ramos, David Fernández-Rodríguez, Inmaculada  
549 González-García, “High-pressure versus low-pressure exhaust gas recirculation in  
550 a Euro 6 diesel engine with lean-NOx trap: Effectiveness to reduce NOx emissions”  
551 International Journal of Engine Research 20 (1) (2018) 155-163  
552 <https://doi.org/10.1177/1468087418817447>.
- 553 23. Thangaraja, J., Kannan, C., “Effect of exhaust gas recirculation on advanced diesel  
554 combustion and alternate fuels - A review.” Applied Energy 180 (2016) 169-184.
- 555 24. José Manuel Luján, Carlos Guardiola, Benjamín Pla, Alberto Reig. “Switching  
556 strategy between HP (high pressure) – and LPEGR (low pressure exhaust gas  
557 recirculation) systems for reduced fuel consumption and emissions.” Energy 90  
558 (2015) 1790-1798.
- 559 25. J.R. Serrano, P. Piqueras, R. Navarro, D. Tarí, C.M. Meano, “Development and  
560 verification of an in-flow water condensation model for 3D-CFD simulations of humid  
561 air streams mixing.” Computers and Fluids 167 (2018) 158-165.
- 562 26. J. Galindo, P. Piqueras, R. Navarro, D. Tarí, C.M. Meano, “Validation and sensitivity  
563 analysis of an in-flow water condensation model for 3D-CFD simulations of humid air

- 564 streams mixing” International Journal of Thermal Sciences 136 (2019) 410-419.  
565 <https://doi.org/10.1016/j.ijthermalsci.2018.10.043>.
- 566 27. J. M. Luján, V. Dolz, J. Monsalve-Serrano, M. A. Bernal Maldonado, “High-pressure  
567 exhaust gas recirculation line condensation model of an internal combustion diesel  
568 engine operating at cold conditions” International Journal of Engine Research (2019)  
569 <https://doi.org/10.1177/1468087419868026>.
- 570 28. Robert M. Siewert, Roger B. Krieger, Mark S. Huebler, Prafulla C. Baruah, Bahram  
571 Khalighi and Markus Wesslau, “Modifying and Intake Manifold to Improve Cylinder-  
572 to-Cylinder EGR Distribution in a DI Diesel Engine Using Combined CFD and Engine  
573 Experiments” 2001 SAE Technical Paper 2001-01-3685,  
574 <http://dx.doi.org/10.4271/2001-01-3685>.
- 575 29. William P. Partridge, Samuel A. Lewis, Michael J. Ruth, George G. Muntean, Robert  
576 C. Smith and John H. Stang, “Resolving EGR Distribuion and Mixing”, 2002, SAE  
577 Technical Paper 2002-01-2882, <http://dx.doi.org/10.4271/2002-01-2882>.
- 578 30. Alain Maiboom, Xavier Tazua and Jean-François Hétet, “Influence of EGR unequal  
579 distribution from cylinder to cylinder on NOx-PM trade-off of a HSDI automotive  
580 Diesel engine” Applied Thermal Engineering 29 (2009) 2043-2050,  
581 doi:10.1016/j.applthermaleng.2008.10.017
- 582 31. Alain Maiboom, Xavier Tazua, Samiur Rahman Shah, Jean-François Hétet.  
583 “Experimental Study of an LP EGR System on an Automotive Diesel Engine,  
584 compared to HP EGR with respect to PM and NOx Emissions and Specific Fuel  
585 Consumption” SAE Int. J. Engines 2(2):597-610, 2010, doi:10.4271/2009-24-0138.
- 586 32. F. Payri, JM Luján, H Climent, B. Pla, “Effects on the intake charge distribution in  
587 HSDI engines”, 2010, SAE Technical Paper 2010-01-1119,  
588 <http://dx.doi.org/10.4271/2010-01-1119>
- 589 33. Hardik Lakhiani, Jyotirmoy Barman, Karan Rajput and Angshuman Goswami,  
590 “Experimental Study of EGR Mixture Design and its Influence on EGR Distribution  
591 Across the Cylinder for NOx-PM Tradeoff” 2013 SAE Int. doi: 10.4271/2013-01-  
592 2743.
- 593 34. Pavlos Dimitriou, Richard Burke, Colin Copeland, Sam Akehurst, “Study on the  
594 Effects of EGR Supply Configuration on Cylinder-to-Cylinder Dispersion and Engine  
595 Performance Using 1D-3D Co-Simulation” 2015 SAE Int.
- 596 35. José Manuel Luján, Héctor Climent, Benjamín Pla, Manuel Eduardo Rivas-Perea,  
597 Nicolas-Yoan François, Jose Borges-Alejo, Zoulikha Soukeur, “Exhaust gas  
598 recirculation dispersión analysis using in-cylinder pressure measurements in  
599 automotive diesel engines” Applied Thermal Engineering 89 (2015) 459-468,  
600 <http://dx.doi.org/10.1016/j.applthermaleng.2015.06.029>.
- 601 36. J.M. Luján, H. Climent, L.M. García Cuevas, A. Moratal, “Volumetric efficiency  
602 modelling of internal combustion engines based on a novel adaptative learnig  
603 algorithm of artificial neural networks” Applied Thermal Engineering 123 (2017) 625-  
604 634.